S 33017 *AMES GRANT*
IN-02-CR
8220
P.10

POWER-ON PERFORMANCE PREDICTIONS FOR A COMPLETE GENERIC HYPERSONIC VEHICLE CONFIGURATION

Dr. Bradford C. Bennett

POWER-ON PERFORMANCE PREDICTIONS FOR A COMPLETE GENERIC HYPERSONIC VEHICLE CONFIGURATION

Dr. Bradford C. Bennett

Power-On Performance Predictions for a Complete Generic Hypersonic Vehicle Configuration

Bradford Bennett

INTRODUCTION

Interest in hypersonic inlets has been spurred by the National Aero-Space Plane (NASP) and the high-speed transport programs. Several computational fluid dynamic (CFD) solutions[1,2] to hypersonic sonic inlet flows have been presented in the last few years. However, because of the complex nature of these internal flows, the computations have required many hours of supercomputing time for a single solution. For CFD to have a significant impact on the design of hypersonic inlets, as well as on the overall design of a hypersonic air-breathing vehicle, computations must be economical.

The Compressible Navier-Stokes (CNS) code was developed to compute external hypersonic flow fields. It has been applied to various hypersonic external flow applications.[3,4,5] In this study, CNS code was modified to compute hypersonic internal flow fields. Calculations were performed on a Mach 18 sidewall compression inlet and on the Lewis Mach 5 inlet. The use of the ARC3D diagonal algorithm (CNS was developed using the F3D algorithm) was evaluated for internal flows on the Mach 5 inlet flow.

The initial modifications to CNS code involved generalization of the boundary conditions and the addition of viscous terms in the second crossflow direction and modifications to the Baldwin-Lomax turbulence model for corner flows. These changes were initially validated by calculations of laminar Mach 18 helium flow in a sidewall compression inlet. The flow conditions were set to model an experiment performed by Carl Trexler. These changes to CNS and the computations described above are outlined in detail in Appendix A.

Mach 5 Inlet

The experimental inlet is a scale model of a proposed Mach 5 aircraft mixed-compression inlet, see Figure 1. The inlet was

1

tested in the NASA Lewis 10 x 10 Supersonic Wind Tunnel. Because the maximum Mach number which can be achieved in this wind tunnel is 3.5, the inlet was oriented with a negative angle of attack of 8.5 degrees so that the flow entering the inlet goes through an expansion on the precompression ramp to a Mach number of about 4.1. The total tunnel pressure was 35.4 psi and the Reynolds number was 8.17×10^6 per meter. A series of three ramps generate oblique shock waves external to the cowl. The cowl generates an oblique shock inside the inlet, which reflects from the ramp surface and terminates in a normal shock downstream of the inlet throat. A subsonic diffuser further compresses the flow and takes it to an exit duct. This study deals only with the supersonic portion of the flow upstream of the normal shock. Grit was applied to the precompression ramp to initiate turbulent flow in the inlet.

Figure 2 shows the locations of the rakes and translating probes in the Mach 5 inlet. There are also numerous surface pressure taps located on the ramp and side walls. Thus, there is a large pool of pitot pressure and surface pressure data available for comparison with computational results.

GRID

The base grid is made of four zones totaling 206,000 points, see Figure 3. The first zone encompasses the upstream area over the precompression ramp. The second zone lies over the downstream part of the precompression ramp and a small portion of ramp 1. Zone 3 is over ramps 1,2 and most of ramp 3. Zone 4 axially covers the same length as zones 1,2, and 3, but lies outside of the inlet. For the initial study, the computations are all upstream of the cowl. The grid in zones 1,2, and 3 is clustered at the ramp and side walls and their uppermost grid lines follow the edge of the side wall.

Since the inlet is symmetric, only half of the inlet flow is computed with a symmetric boundary condition applied on the center plane. A simple extrapolation is applied on the upper boundary of zone 4 and at the outflow boundary of zones 3 and 4. The flow field conditions at the inflow boundary, upstream of the precompression ramp leading edge, are held constant. No-slip conditions are applied at all solid walls. All edges are modeled as being sharp.

2

Preliminary Results

Computations have been performed with both the F3D and ARC3D algorithms. A partially converged solution was obtained using the F3D algorithm, but the time step required for the code to remain stable was so small that 30 cpu hours of Cray YMP time were needed to reduce the L_2 norm of the residual by two orders of magnitude. Figure 4 shows the pressure along the ramp wall centerline. Even at this level of convergence there is good agreement with the experimental wall pressures. Figure 5 shows the pressure contours along the symmetry plane of the inlet. The system of oblique shocks generated by the leading edge and the ramps is clearly seen.

At this point, the ARC3D algorithm was put in CNS. Unfortunately, the ARC3D algorithm is unstable in zone 1 where the leading edge shock is strong. Hence, the F3D algorithm was used in zone 1 and a starting solution was obtained for zone 1 and part of zone 4. The remainder of the flow was calculated using the ARC3D algorithm. The cpu time required per time step with the ARC3D algorithm is approximately one-half that required for the F3D algorithm on this grid. In addition, it is possible to use a time step approximately 5 times as large. Combining the algorithms in this manner only 10 cpu hours were required to obtain convergence equivalent to that obtained using F3D only.

Figure 6 shows that the ARC3D wall pressures along the centerline of the ramp wall agree well with the experimental data. Figures 6 and 7 are comparisons of computed pitot pressures with experimental measurements. Here the comparisons suggest that the boundary layer in the computation is thicker than in the experiment. This could be the result of the differences in the experiment and the inlet boundary conditions.

In the experiment, the flow was expanded around the leading edge of the inlet to increase the Mach number from 3.5 to 4.1. Thus the flow initially accelerates on the precompression ramp. In the computation a constant free stream condition of Mach 4.1 is set at the leading edge of the inlet.

Current Status

The final months of this contract will be spent in examining different methods of accelerating the convergence of the solution. The area of the grid overlap between two adjacent zones will be checked as a possible source of numerical instability. Additional experimental data will be compared to the numerical results that have already been obtained and the differences between the experimental measurements and the numerical results will be studied.

References

1. W. C. Rose, E. W. Perkins, G. W. Howe, and D. P. Bencze, "Analysis of Sidewall Compression Inlets at High Speed (U)," Sixth National Aero-Space Plane Symposium, April, 1989.

2. Reddy, D. R., Benson, T. J., Weir, L. J., "Comparison of 3-D Viscous Flow Computations of Mach 5 Inlet with Experimental Data," AIAA Paper 90-0600, January, 1990.

3. Ryan, J. S., Flores, J., and Chow, C.-Y., "Hypersonic Flow Simulations about the All-body Configuration Using a Zonal Approach," Paper 92, *Fourth National Aero-Space Plane Technology Symposium;* Monterey, CA, February 17-19, 1988.

4. Edwards, T. A., and Flores, J., "Toward a CFD Nose-to-Tail Capability; Hypersonic Unsteady Navier-Stokes Code Validation," AIAA Paper 89-1672, June 12, 14, 1989.

5. Ryan, J. S., Flores, J., and Chow, C.-Y., "Development and Validation of CNS (Compressible Navier-Stokes) for Hypersonic Applications," AIAA Paper 89-1839, June 12-14, 1989.
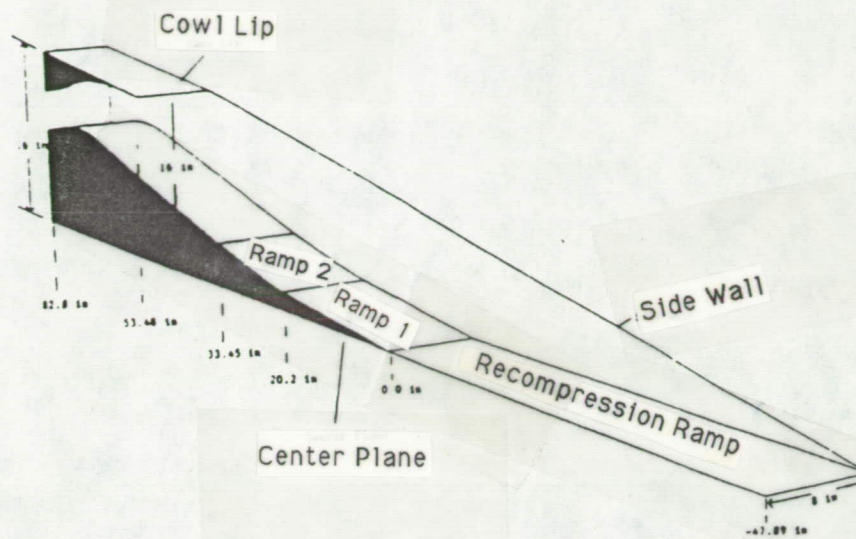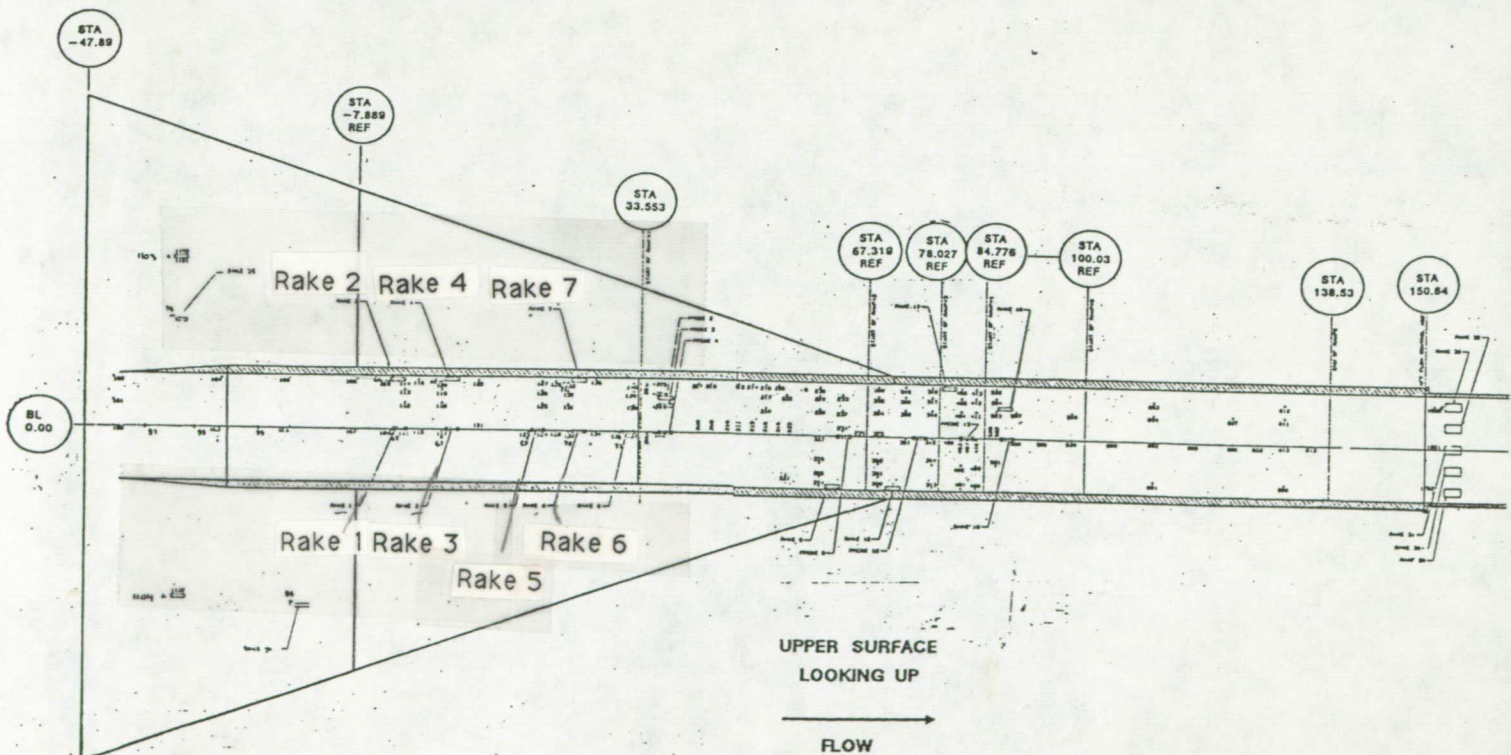
Figure 1. Schematic of Lewis Mach 5 inlet.

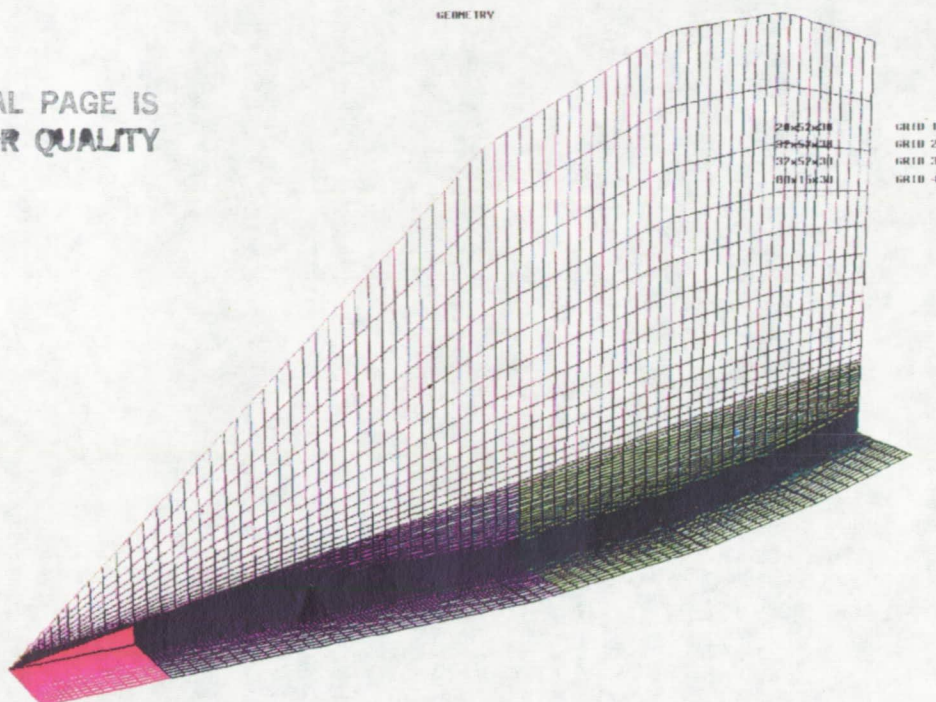Figure 2. Locations of pressure taps and rakes in Mach 5. inlet.

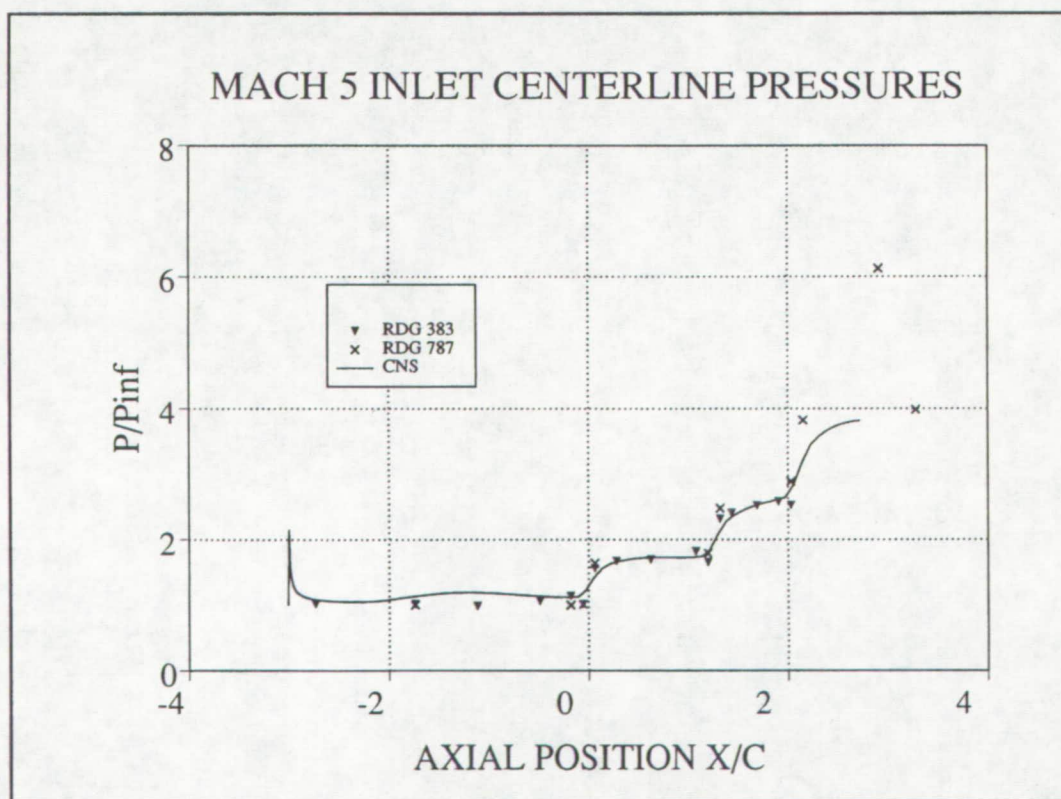Figure 3. Four zone grid used to model Mach 5 inlet.

Figure 4. Comparison of computed (F3D algorithm) and measured ramp wall center-line surface pressures.
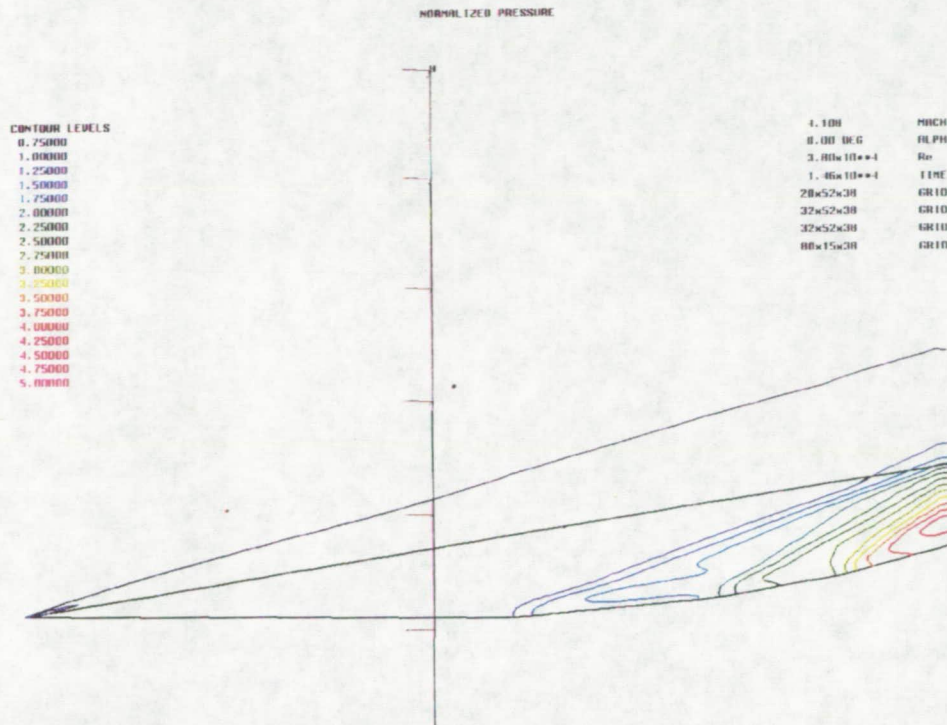
6

Figure 5. Computed pressure contours along the symmetry plane of the Mach 5 inlet using CNS with the F3D algorithm.
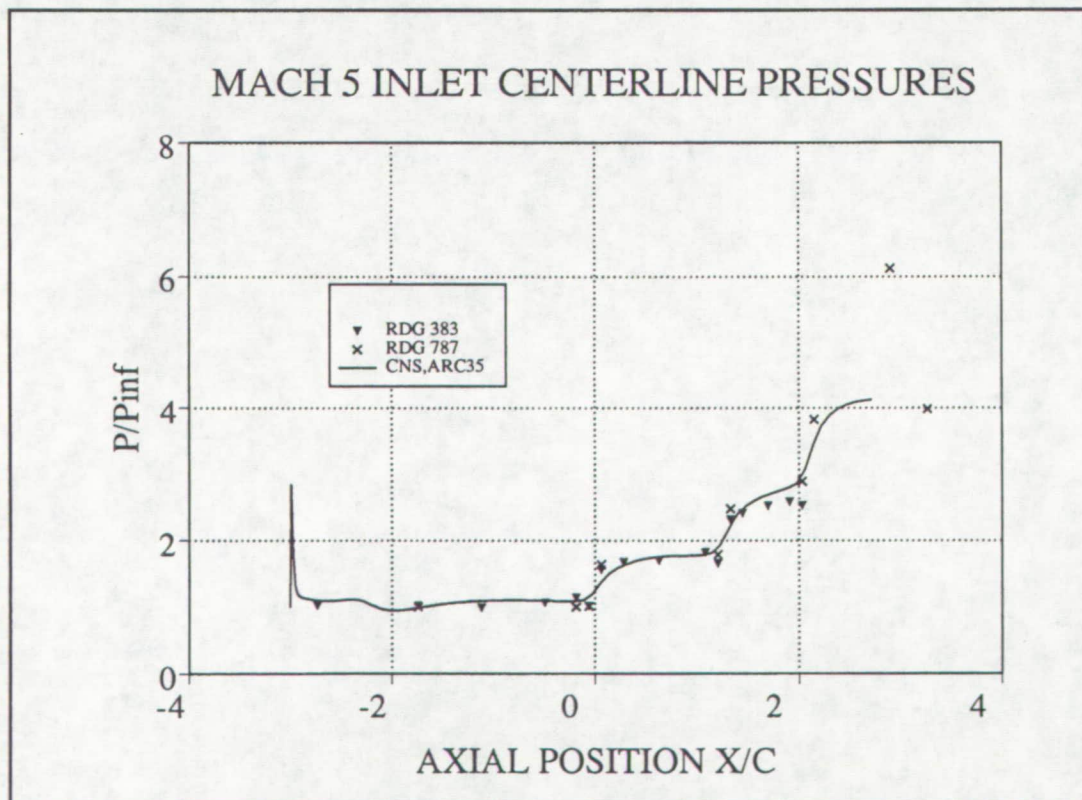

Figure 6. Comparison of computed (ARC3D algorithm) and measured ramp wall centerline surface pressures.
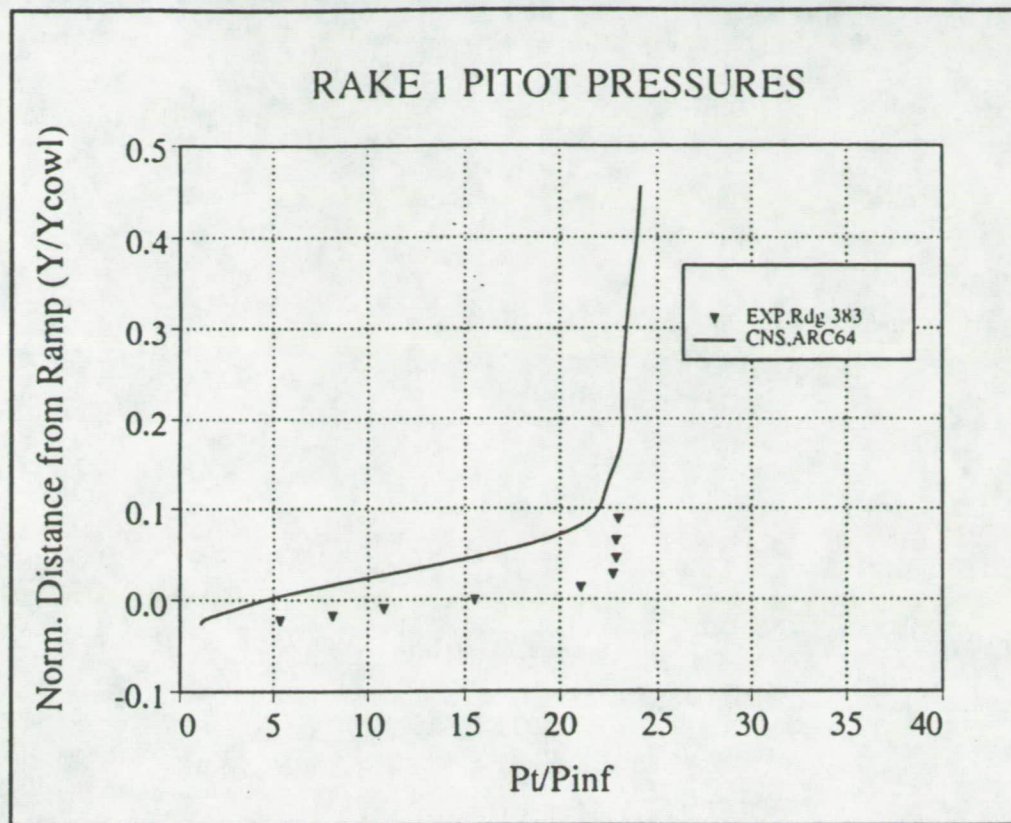
Figure 7. Comparison of computed (ARC3D algorithm) and measured pitot pressures for Rake 1.
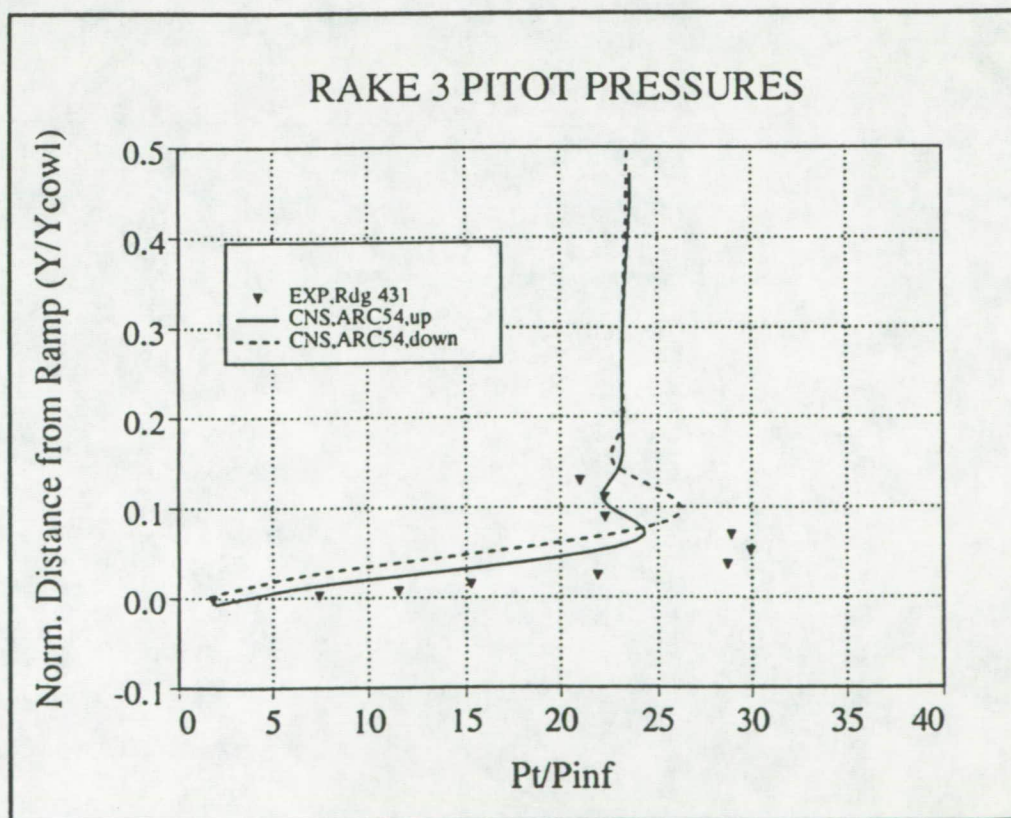

Figure 8. Comparison of computed (ARC3D algorithm) and measured pitot pressures for Rake 3.

8